Time-Dependent Bifurcation in a Dynamical System

Marko Kocic

Bachelor's Thesis in Computer Science
at Stockholm University, Sweden, 2020

Stockholm University

Time-Dependent Bifurcation in a Dynamical System

Marko Kocic

Bachelor's Thesis in Computer Science (15 ECTS credits)
Bachelor's Programme in Computer Science
Stockholm University year 2020
Supervisor at the Department of Mathematics was Woosok Moon
Examiner was Lars Arvestad

Department of Mathematics
Stockholm University
SE-106 91 Stockholm, Sweden

Abstract

This paper analyses the mathematical model used when treating the Arctic sea-ice in climate science. Global warming and the increase of greenhouse gases have nearly pushed the Arctic sea-ice system past the critical point, identified by ice-albedo positive feedback. This work establishes a physical model and applies knowledge from bifurcation theory to identify the behaviour of the ice-albedo positive feedback. In particular, one parameter used in bifurcation theory is attributed to a time component, turning the model into a non-autonomous ordinary differential equation. The results, if applicable to the real world scenario, show a system where, if the Arctic sea-ice system is pushed past its critical point, then the speed at which global warming occurs will not matter for the melting. Furthermore, the Arctic sea-ice in any case will melt in a small time window if global warming is not controlled immediately.

Tidsberoende bifurkation i ett dynamiskt system

Sammanfattning

Detta arbete analyserar den matematiska modellen som behandlar Arktiska havsisen i klimatvetenskap. Globala uppvärmningen och ökningen av växthusgaser har nästan tryckt Arktiska havsissystemet förbi den kritiska punkten, vilket beskrivs av is-albedo positiv respons. Arbetet tar modellen och applicerar kunskap från bifurkationsteori för att identifiera beteendet av is-albedo responsen. Mer specifikt, en parameter som används inom bifurkationsteori ges en tidskomponent, vilket förändrar modellen till en ickeautonom ordinär differentialekvation. Resultatet, om tillämpbar till situationen i verkligheten, visar ett system där om Artiska havsisen trycks förbi kritiska punkten kommer inte hastigheten av globala uppvärmningen spela roll för smältningen. Vidare, oavsett situation kommer Artiska havsisen smälta inom en kort period om globala uppvärmningen inte bromsas omedelbart.

Acknowledgements

Special thanks go to my supervisor Woosok Moon for the project idea and for all advises about how to move with the project forward when it stuck. My thanks also go to Mikica Kocic for helpful discussions about physics and verifying the code. Finally, I wish to thank the rest of my family and friends for all direct and indirect support throughout the work.

Contents

Introduction

The increase of greenhouse gases which affect global warming, may push components of the Earth's systems past critical states into different modes of operation; such a scenario would produce a large-scale change in human and ecological systems. One particularly important component is the Arctic sea-ice, which may cause climate ripples and affect other components of the Earth's system such as the Greenland ice sheet [1]. The term *tipping point* is used when small changes cause larger and long-term consequences for a system, and it is relevant on the topic of Arctic sea-ice.

The tipping point for Arctic sea-ice is described by ice-albedo positive feedback: ice melts, causing water to absorb more heat which causes more ice to melt. The Arctic sea-ice is declining at present, and some believe the shrinkage is attributed to ice-albedo positive feedback due to the non-linear shrinkage. Unfortunately, a common critical threshold has not been identified yet, so some believe the tipping point has already been passed and others disagree [1].

A tipping point can be described as an *abrupt climate change*, which is defined as "when the climate system is forced to cross some threshold, triggering a transition to a new state at a rate determined by the climate system itself and faster than the cause" [1]. Mathematically, the term "tipping point" denotes a case of bifurcation, which focuses on equilibrium properties and implies some degree of irreversibility (points of no returns). As such, numerical methods for dynamical systems may be used in the analysis of the tipping point, wherever it may be.

This work analyses the bifurcation theory of the dynamical system which describes the melting of the Arctic sea-ice. The primary issue which arises is that bifurcation theory does not cover the Arctic sea-ice model perfectly. The bifurcation parameter used to examine the steady-state solutions for the climate model is time-dependent, which is different from normal bifurcation theory. Subsequently, the work focuses on the time-dependent bifurcation transition aspect, which occurs in real-life, and attempts to conclude what may occur if global warming is left unchecked.

1 A brief introduction to the climate change

The idea behind this section is to give an overview of how a climate change occurs and what is relevant to explain a time-dependent bifurcation in the dynamical system that is the Arctic sea-ice.

1.1 Conceptual physics behind the climate change

We begin by exploring the physics involved in climate change [2]. The most important physical processes are the absorption and reflection of energy, and how the greenhouse effect changes the absorption/reflection dynamic. Further we identify the issue with global warming and how it relates to the physical process of absorption and reflection of energy.

1.1.1 Absorption and reflection of energy

The Sun heats the Earth through radiation. This energy, also known as radiant energy, is in the form of electromagnetic waves. Every physical object emits radiant energy directly proportional to the temperature of the emitter. The Sun emits large amounts of radiant energy that is concentrated mostly in the visible light spectrum. On the other hand, regular everyday objects (such as animals, trees, water, or the Earth) radiate far less energy. Moreover, their radiant energy lies in the infrared spectrum.

As every object is emitting radiant energy, every object also absorbs radiant energy. Good emitters of radiant energy are also good absorbers; bad emitters are also bad absorbers. This follows from Kirchhoff's law of thermal radiation which states that the emissivity is equal to the absorptivity for an arbitrary body in thermodynamic equilibrium.

A simple showcase of objects which are good or bad absorbers can be done by filling two identical cups with boiling water and placing the cups in room temperature. Let us say the two cups are differently coloured, one is black and the other one is white or mirror-like. The black cup will cool down faster, as it is a good emitter of radiant energy. At the same time, we also have a reflection of radiant energy. Reflection and absorption are opposite processes: a good absorber is a bad reflector, and a bad absorber is a good reflector. In connection with the earlier example, white and mirror-like objects reflect energy better. That is to say, white objects such as fresh snow reflect energy while the darker water absorbs energy.

Reflexivity of an object can be described by a unit called *albedo*. An albedo is a dimensionless unit which describes how much of the energy is reflected. Higher albedo implies higher reflexivity and lower albedo implies lower reflexivity, and by consequence, higher absorption. Hence, fresh snow has a high albedo, while water has a low albedo.

1.1.2 The greenhouse effect

The greenhouse effect is a physical process which is keeping the Earth at a comfortable temperature for humans. Without greenhouse gases the Earth would be considerable colder and entirely different from what we recognise.

The greenhouse effect is easily explained as follows. Consider a greenhouse made of glass, which is exposed to the sunlight. Glass is transparent to visible and near-infrared light, while it is opaque to the far-infrared radiation. The Sun, due to its high temperature emits high-frequency radiation which the glass considers transparent, heating the inside of the greenhouse very well. On the other hand, objects inside the greenhouse emit low-frequency (far-infrared) radiation which does not pass through the glass. This process results in trapping the radiation, making the inside of the greenhouse even warmer.

A similar process happens to the Earth, where the gases H_2O (water vapour) and CO_2 (carbon dioxide) in the atmosphere act as the glass-wall. While H_2O is the primary greenhouse gas, the human contributed increase of CO_2 is growing alarmingly quickly and may even contribute to H_2O increase. Nonetheless, the increasing CO_2 is a major concern and needs to be controlled quickly.

1.1.3 Climate change and tipping point

The primary issue with an increase in greenhouse gases is global warming, or rather its consequence—climate change. The Earth system has many components sensitive to small changes; a change in one of the systems will cause a change in another. Even worse is that a few of these systems are sensitive for abrupt climate change, which can be defined as "when the climate system is forced to cross some threshold, triggering a transition to a new state at a rate determined by the climate system itself and faster than the cause" [1]. Such abrupt climate changes can be described to have tipping elements; a small perturbation may cause subsystems of the Earth system to be switch into a qualitatively different state.

As a tipping point can be considered the moment when the abrupt climate change is caused. Many of the subsystems of the Earth are subject to climate change, but many of the systems also do not have a convincingly established tipping point. Even then, a list of potential future tipping elements has been established. Among these elements are the Amazon rainforest, the Greenland ice sheet, the Boreal forest in Canada, the Russian tundra, and finally, the one which is important for this paper: the Arctic sea-ice.

The Arctic sea-ice is one of the subsystems which does not have an established tipping point, yet the sea-ice is shrinking at a faster-than-linear rate in the last 30 years. The cause for Arctic sea-ice shrinking is easier to identify, however, and has been attributed to ice-albedo positive feedback. The ice-albedo positive feedback is defined to be a process of ice melting quicker due to the reduction in albedo. As the snow sheet on ice melts to water the new water (which has a much lower albedo) absorbs more radiation, which in turn heats the surroundings of the ice leading to even more ice melting. The reverse process exists too: ice-albedo negative feedback

causing more ice to freeze due to the higher albedo of ice and snow, reflecting more light causing more ice to form. Nonetheless, the ice-albedo positive feedback is of major concern regarding the melting of Arctic sea-ice, and the process may be very fast if the current trend of global warming stays the same.

The concern with Arctic sea-ice tipping point is also the implication of a point of no return. If the Arctic sea-ice melts, immediate consequences will be visible in the Greenland ice sheet, the Russian tundra, and the Gulf stream. Unfortunately, while the existence of a tipping point and its consequences is well understood, it is not as easy to pinpoint when and how the system will tip past the critical point.

1.2 Mathematical model

Here we put the physical concepts from section 1.1 into a mathematical model that is used in climate science [3]; initially, interest about such models was sparked by the independent results of Budyko [4] and Sellers [5–7] in the late 1960's.

Radiation from the Sun is energy heating up the surface area of the Earth in a certain amount of time. Computing the units $\mathrm{J\ s^{-1}} = \mathrm{W}$ over surface area $\mathrm{m^2}$ gives $\mathrm{W\ m^{-2}}$. An estimated value of the solar radiance is [8],

$$S = (1360.8 \pm 0.5)\ \mathrm{W\ m^{-2}}. \tag{1.1}$$

Assuming the Earth to be a ball of radius r, then the Earth's surface area is given by $4\pi r^2$. Further we can assume that solar energy hitting the Earth is a disc with the same radius as of the Earth's. Hence, the result becomes,

$$J_{\text{in}} = \frac{1}{4} S, \tag{1.2}$$

since the solar energy is being spread all over the Earth's surface.

Not all of the radiant energy will be absorbed by the Earth's surface, so we need the albedo of the Earth's surface. Remember that albedo α is a dimensionless unit, which we will now define as a number such that $0 < \alpha < 1$. However, since higher albedo implies high reflexivity, we need how much it absorbs; this is given by the factor $1 - \alpha$. Including this factor, (1.2) becomes,

$$J_{\text{in}} = \frac{1}{4} S\,(1 - \alpha). \tag{1.3}$$

On the other hand, we can consider the Earth as a black body with its own radiation. The outgoing radiance is given by the Stefan-Boltzmann law,

$$J_{\text{out}} = \sigma T^4, \tag{1.4}$$

where T is the black body temperature while σ is Stefan-Boltzmann constant [9],

$$\sigma = \frac{2\pi^5}{15} \frac{k^4}{c^2 h^3} = 5.670374419... \times 10^{-8}\ \text{(exact)}\ \frac{\mathrm{W}}{\mathrm{m^2\,K^4}},$$

where k is the Boltzmann constant, h is the Planck constant, and c is the speed of light in vacuum. Nevertheless, due to factors such as clouds the Earth cannot be considered a perfect black body. Subsequently, we modify equation (1.4) to,

$$J_{\text{out}} = \lambda\, \sigma T^4, \tag{1.5}$$

where λ is a dimensionless unit such that $0 < \lambda < 1$.

Another physical process (briefly mentioned in section 1.1) is that the temperature between two objects eventually seek to a common equilibrium. In simple terms, it is when the outgoing radiance is equal to the ingoing radiance. The equilibrium of Earth's temperature is therefore given when (1.3) and (1.5) are equal, that is to say,

$$J_{\text{in}} = J_{\text{out}} \quad \Leftrightarrow \quad \frac{1}{4} S\,(1-\alpha) = \lambda\, \sigma T^4 \quad \Leftrightarrow \quad 0 = \frac{1}{4} S\,(1-\alpha) - \lambda\, \sigma T^4. \tag{1.6}$$

A solution to the equation (1.6) is the mean temperature of the surface of the Earth. Whenever equations (1.3) and (1.5) are not equal, there is a gain or loss of heat of the Earth's surface. The temperature change is obtained from $C_p \mathrm{d}T = \mathrm{d}Q$, where Q is the heat energy added to the system, and $C_p \mathrm{d}T/\mathrm{d}t \propto J_{\text{in}} - J_{\text{out}}$, which gives the zero-dimensional energy balance model [3, sec. 3.2.1],

$$\bar{C}_p \frac{\mathrm{d}T}{\mathrm{d}t} = \frac{1}{4} S\,(1-\alpha) - \lambda\, \sigma T^4. \tag{1.7}$$

Here, $\bar{C}_p$ is the heat capacity of the atmosphere normalized per unit area.

Notwithstanding, the albedo α is typically not constant; it changes depending on how much heat there exists on the surface of the Earth. Lower temperatures freezes the water giving ice sheets and increases the albedo while higher temperature melts the water and decreases the albedo. As such, it is suitable to view the albedo as a function of temperature. This gives the one-dimensional model [3, sec. 3.2.2],

$$\bar{C}_p \frac{\mathrm{d}T}{\mathrm{d}t} = \frac{1}{4} S\left(1-\alpha(T)\right) - \lambda\, \sigma T^4. \tag{1.8}$$

Extensions. We can also introduce the external parameter ΔF which represents the greenhouse effect of the atmosphere. It is easiest to consider the atmosphere to keep a flat amount of the radiance such that,

$$\bar{C}_p \frac{\mathrm{d}T}{\mathrm{d}t} = \frac{1}{4} S\left(1-\alpha(T)\right) - \lambda\, \sigma T^4 + \Delta F. \tag{1.9}$$

This is a complete model of the climate that will be used in the rest of the paper. Similarly to albedo, the ΔF parameter is also suitable to be viewed as a function, but of time instead of temperature. Hence, the time-dependent variant of (1.9) reads,

$$\bar{C}_p \frac{\mathrm{d}T}{\mathrm{d}t} = \frac{1}{4} S\left(1-\alpha(T)\right) - \lambda\, \sigma T^4 + \Delta F(t). \tag{1.10}$$

The models (1.9) and (1.10) will be extensively used throughout the paper.

2 Bifurcation theory

Bifurcation theory of differential equations is the study of changes in their solutions. In general, a differential equation may be dependent on some external parameters. As these parameters change, the qualitative behaviour of the solutions may also change; for example, the number of distinct solutions or their stability may vary from point to point in a parameter space. Points where the behaviour of the solutions change are called *bifurcation points* [10]. In this section we tackle three types of bifurcations: a saddle-node bifurcation, a normal transcritical bifurcation, and a time-dependent transcritical bifurcation. Here we also show bifurcation diagrams for some toy models. In the later sections we shall apply the knowledge to the real-world models given in (1.9) and (1.10).

2.1 Mathematical background

Consider a nonlinear system of ordinary differential equations (ODE),

$$\dot{\boldsymbol{x}} = \frac{\mathrm{d}\boldsymbol{x}}{\mathrm{d}t} = \boldsymbol{f}(\boldsymbol{x};\boldsymbol{a}), \tag{2.1}$$

with a state variable $\boldsymbol{x} = \boldsymbol{x}(t)$. Here, $\boldsymbol{x} = (x_1, \ldots, x_n)$ and $\boldsymbol{f} = (f_1, \ldots, f_n)$ are n-dimensional vectors, and $\boldsymbol{a} = (a_1, \ldots, a_p)$ is a set of parameters. At first, we assume that $\boldsymbol{f}$ does not depend explicitly on t, that is, the system is autonomous.

The system (2.1) can always be enlarged by adding the parameters $\boldsymbol{a}$ into the list of dependent variables $\boldsymbol{x}$ and then supplementing (2.1) with $\dot{\boldsymbol{a}} = \mathrm{d}\boldsymbol{a}/\mathrm{d}t = 0$ to keep the parameters constant.

The configuration space of (2.1) consists of all possible values of the state variable $\boldsymbol{x}$, the phase space consists of all possible solutions $(\boldsymbol{x}, \dot{\boldsymbol{x}})$, and the parameter space consists of all possible values of $\boldsymbol{a}$. The fixed points of the system satisfy $\mathrm{d}\boldsymbol{x}/\mathrm{d}t = 0$, i.e., they are the solutions of the equation $\boldsymbol{f}(\boldsymbol{x};\boldsymbol{a}) = 0$, in other words, they are points where the vector field $\boldsymbol{f}$ vanishes in the phase diagram. On a side note, it is worth mentioning that the change of variables $\boldsymbol{x} = \boldsymbol{x}_{\mathrm{ref}} + \boldsymbol{y}$ transforms any arbitrary solution $\boldsymbol{x}_{\mathrm{ref}}$ of (2.1) into a steady-state solution of the new system, $\dot{\boldsymbol{y}} = \boldsymbol{f}(\boldsymbol{x}_{\mathrm{ref}} + \boldsymbol{y};\boldsymbol{a}) - \dot{\boldsymbol{x}}_{\mathrm{ref}}$, where $\boldsymbol{f}(\boldsymbol{x}_{\mathrm{ref}};\boldsymbol{a}) = \dot{\boldsymbol{x}}_{\mathrm{ref}}$ corresponds to $\dot{\boldsymbol{y}} = 0$ with the fixed point $\boldsymbol{y} = 0$. This is very useful and employed in the perturbation theory.

The Jacobian matrix of the system reads,

$$\mathbf{J}(\boldsymbol{x};\boldsymbol{a}) \coloneqq \frac{\partial \boldsymbol{f}(\boldsymbol{x};\boldsymbol{a})}{\partial \boldsymbol{x}}, \tag{2.2}$$

with the matrix elements $J_{ij} = \partial f_i(x_1, ..., x_n; a_1, ...a_p)/\partial x_j$. Using the solution $\boldsymbol{x}(t;\boldsymbol{a})$ of (2.1), bifurcation points are the values of the parameters $\boldsymbol{a}$ where one or more eigenvalues of the Jacobian matrix $\mathbf{J}$ are zero [10]. Considering only the steady-state solutions (i.e., the fixed points), the bifurcation points satisfy the compound system,

$$\boldsymbol{f}(\boldsymbol{x};\boldsymbol{a}) = 0, \qquad \det \mathbf{J}(\boldsymbol{x};\boldsymbol{a}) = 0. \tag{2.3}$$

At bifurcation points, the number of the solutions and the stability of the solutions may change. The solution is said to be stable if small perturbations in the initial conditions or parameters lead to small changes in the solution. More precisely, a solution $\boldsymbol{x}(t)$ of the system (2.1) is said to be stable if, for all $\epsilon > 0$ there exists $\delta > 0$ such that any solution $\boldsymbol{y}(t)$ satisfying $|\boldsymbol{y}(0) - \boldsymbol{x}(0)| < \delta$ also satisfies $|\boldsymbol{y}(t) - \boldsymbol{x}(t)| < \epsilon$.

As known, the stability of a solution is governed by the eigenvalues of the Jacobian [10]. In particular, the solution is unstable if any of the eigenvalues has a positive real part. If the system has a highly nonlinear $\boldsymbol{f}$, investigating eigenvalues of the Jacobian can become very complicated. An alternative approach is to do a small perturbation of an existing (steady-state) solution and then examine the linear stability of those (perturbed) solutions.

We now sketch a procedure how to examine the linear stability of an existing solution $x_0(t)$ for the one-dimensional differential equation $\dot{x} = f(x; a)$. For this purpose, a perturbation series expansion around x_0 is employed where $\varepsilon \to 0$ [11],

$$x(t) = x_0(t) + \varepsilon x_1(t) + \varepsilon^2 x_2(t) + \dots \quad . \tag{2.4}$$

Substitution into (2.1) yields the following equations to orders ε^0, ε^1, ε^2, ...,

$$\dot{x}_0 = f(x_0; a), \tag{2.5}$$
$$\dot{x}_1 = x_1 f'(x_0; a), \tag{2.6}$$
$$\dot{x}_2 = x_2 f'(x_0; a) + x_1^2 f''(x_0; a), \quad \dots \quad . \tag{2.7}$$

Since the existing solution x_0 already satisfies (2.5), we need to solve and analyse the linear perturbation x_1 from the first-order equation (2.6). Any exponential growth or divergence of x_1 indicates that x_0 is unstable. Note that linear stability does not imply the full (nonlinear) stability at all orders [11].

As an illustration of the presented theoretical concepts, in the following subsections we will explore a few cases by example.

2.2 Saddle-node bifurcation

We begin with a saddle-node bifurcation, also known as a fold bifurcation; in this case two solutions fold together to remove both of the solutions. As an example, consider a simple one-dimensional dynamical system,

$$\frac{\mathrm{d}x}{\mathrm{d}t} = f(x; a) = a - x^2, \tag{2.8}$$

where a is an externally tuned parameter and $x, a \in \mathbb{R}$. The Jacobian of (2.8) reads,

$$\det J = -2x. \tag{2.9}$$

A steady-state solution is obtained when $\mathrm{d}x/\mathrm{d}t = 0$, yielding the fixed points,

$$x_\mathrm{o} = \pm\sqrt{a}. \tag{2.10}$$

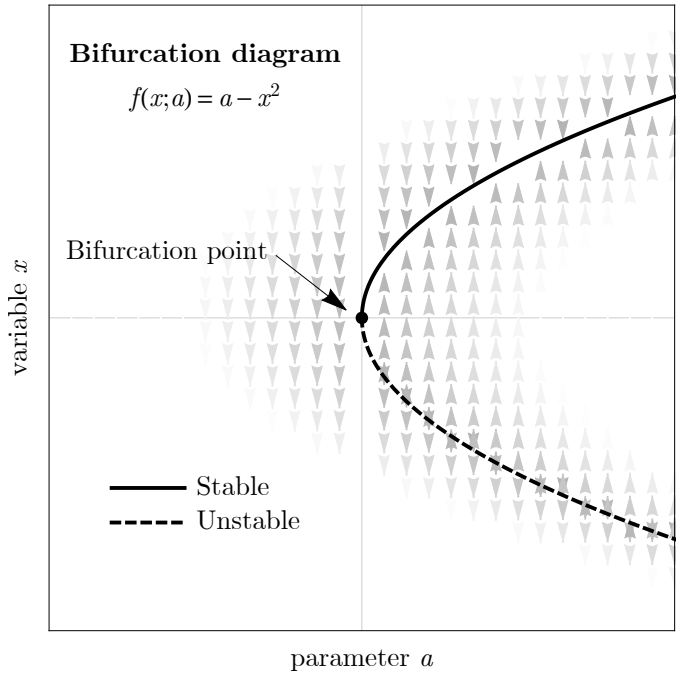

Figure 1: *Steady-state solutions of $\dot{x} = a - x^2$ for different values of a.*

There are two cases: for $a < 0$ there are no real solutions, and for $a > 0$ there exists two real solutions. The Jacobian eigenvalues have a negative real part when $x_\mathrm{o} = \sqrt{a} > 0$, in which case the system is stable. The bifurcation points are obtained from (2.3): $x_\mathrm{o} = \pm\sqrt{a}$, $-2x_\mathrm{o} = 0$, which yields one bifurcation point at $a = 0$.

Let us consider the case $a > 0$. The linear stability of (2.8) can be deduced by analysing (2.6). In our example $f(x; a) = a - x^2$, and the steady-state solutions are $x_\mathrm{o} = \pm\sqrt{a}$; denoting the first-order perturbation in (2.6) by $\eta \coloneqq x_1$, we have,

$$\frac{\mathrm{d}\eta}{\mathrm{d}t} = -2x_\mathrm{o}\,\eta. \tag{2.11}$$

Consequently, a solution in the first order reads,

$$\eta(t) = \eta_0 \exp(-2x_\mathrm{o}\,t). \tag{2.12}$$

Depending on the sign of x_o, we have two cases at $t \to \infty$,

- $\eta \to 0$ for $x_\mathrm{o} = +\sqrt{a} > 0$ (a stable solution), and
- $|\eta| \to \infty$ for $x_\mathrm{o} = -\sqrt{a} < 0$ (an unstable solution).

Finally, we include the parameter a in the configuration space, (a, x), and plot the phase space of the vector field $(\dot{a}, \dot{x}) = (0, a - x^2)$; the result is shown in figure 1. The steady-state solutions for different values of a and the bifurcation point at $a = 0$ are highlighted in the same figure.

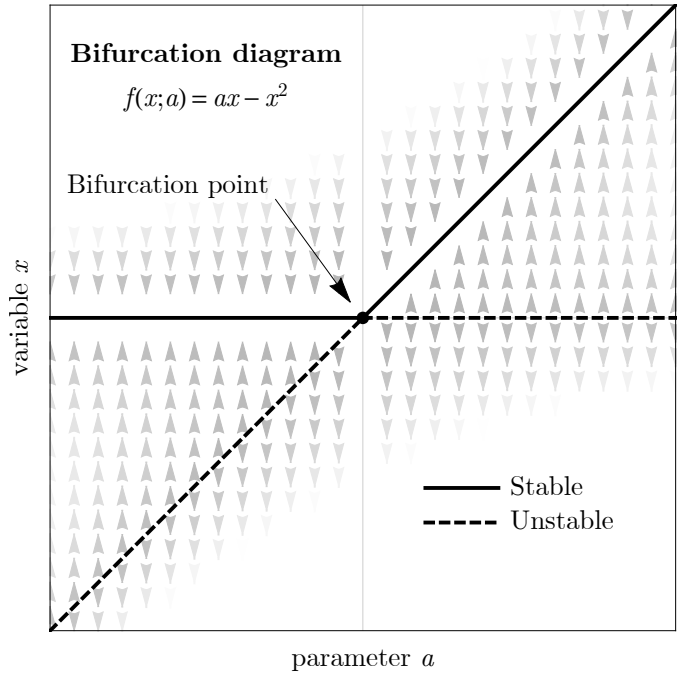

Figure 2: *Steady-state solutions of $\dot{x} = ax - x^2$ for different values of a.*

2.3 Transcritical bifurcation

As our next example, consider the differential equation,

$$\frac{\mathrm{d}x}{\mathrm{d}t} = f(x;a) = ax - x^2. \tag{2.13}$$

This equation is similar to the logistic equation [12], but here we allow a and x to be both positive or negative reals. The equation (2.13) has the following exact solution,

$$x(t) = \frac{a\,\mathrm{e}^{at}}{\mathrm{e}^{at} + c}, \tag{2.14}$$

where c is an integration constant. The Jacobian 'matrix' is $J = a - 2x$, while the steady-state solutions are given by,

(i) $x_{\mathrm{o}1} = 0$ for all $a \in \mathbb{R}$, and
(ii) $x_{\mathrm{o}2} = a$ for all $a \in \mathbb{R}$.

The bifurcation points are solved from $J = a - 2x_{\mathrm{o}} = 0$, yielding $a = 0$. Analysing the eigenvalues of the Jacobian, we conclude that (i) the fixed point $x_{\mathrm{o}1} = 0$ is stable for $a < 0$ and unstable for $a > 0$, and (ii) the fixed point $x_{\mathrm{o}2} = a$ is stable for $a > 0$ and unstable for $a < 0$. The combined result can be viewed in figure 2. Note that we can consider $a = 0$ as the tipping point for this dynamical system, which is of particular interest in the next section.

According to (2.6), the first-order perturbation equation for $\eta \coloneqq x_1$ reads,

$$\frac{\mathrm{d}\eta}{\mathrm{d}t} = (a - 2x_\mathrm{o})\,\eta, \tag{2.15}$$

The first-order solution is,

$$\eta(t) = \eta_0 \exp\Big((a - 2x_\mathrm{o})\,t\Big), \tag{2.16}$$

where x_o is either $x_{\mathrm{o}1} = 0$ or $x_{\mathrm{o}2} = a$. Hence, the linear perturbation confirms the earlier obtained result, where we have,

- a stable solution for $x_{\mathrm{o}1} = 0$ when $a < 0$,
- a stable solution for $x_{\mathrm{o}2} = a$ when $a > 0$,
- an unstable solution for $x_{\mathrm{o}1} = 0$ when $a > 0$,
- an unstable solution for $x_{\mathrm{o}2} = a$ when $a < 0$.

2.4 Time-dependent transcritical bifurcation

Here we modify the transcritical bifurcation example (2.13) by adding a time dependence to the parameter a, that is, we consider $a(t)$. This modification results in a manifestly non-autonomous ODE. To keep the analysis simple, let us take,

$$a(t) = a_0 + At, \tag{2.17}$$

where $A > 0$ is a positive real constant and $a_0 = -1$. This allows setting $\dot{a} = A$, which converts the model back to be autonomous. In summary, we investigate the set of differential equations,

$$\frac{\mathrm{d}x}{\mathrm{d}t} = ax - x^2, \qquad \frac{\mathrm{d}a}{\mathrm{d}t} = A, \tag{2.18}$$

where x and a are time-dependent state variables and $A > 0$ is a free parameter. The initial condition are $a_0 = -1$ and $x_0 > 0$. Then, for a small A where also x_0 is close to zero, we have a slow passage near an earlier steady bifurcation at $a = 0$.

The solution to (2.18) is easily obtained using Mathematica; it reads,

$$x(t) = \frac{\exp(\frac{a^2}{2A})}{c\exp(\frac{a_0^2}{2A}) + \sqrt{\frac{\pi}{2A}}\,\mathrm{erfi}(\frac{a}{\sqrt{2A}})}, \qquad a(t) = a_0 + At. \tag{2.19}$$

Here, c is an integration constant, $\mathrm{erfi}(x)$ is the "imaginary error function" defined as $\mathrm{erfi}(x) \coloneqq -\mathrm{i}\,\mathrm{erf}(\mathrm{i}x)$ where $\mathrm{erf}(x)$ is the error function—a normalized form of the Gaussian function (the probability density function of the normal distribution) [13].

The Jacobian of of the system (2.18) is singular, so we rather do a qualitative analysis using phase diagrams. The vector field and the stream plot are shown in figure 3. In both plots we have used $A = 0.1$ and $a_0 = -1$. These plots also include examples of several solutions and their common asymptotes.

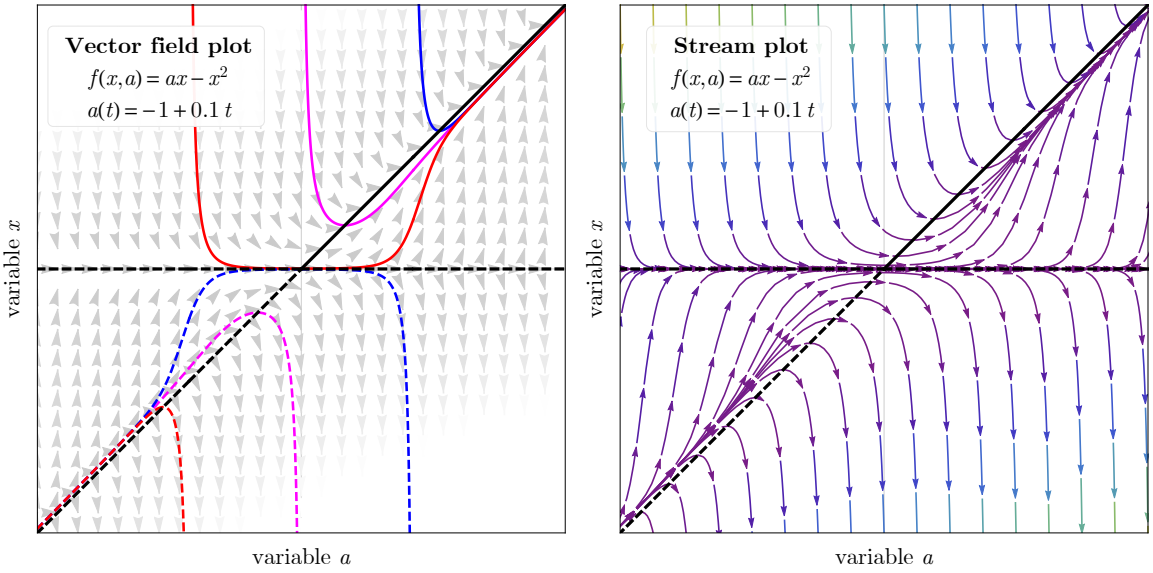

Figure 3: *The vector field and the stream plot for the system (2.18) where $A = 0.1$. The left panel shows several solution examples and their common asymptotes (one stable and one unstable). The stable fixed point from figure 2 for $a < 0$ at $x = 0$, is now pushed towards the infinity and converted into an unstable asymptote.*

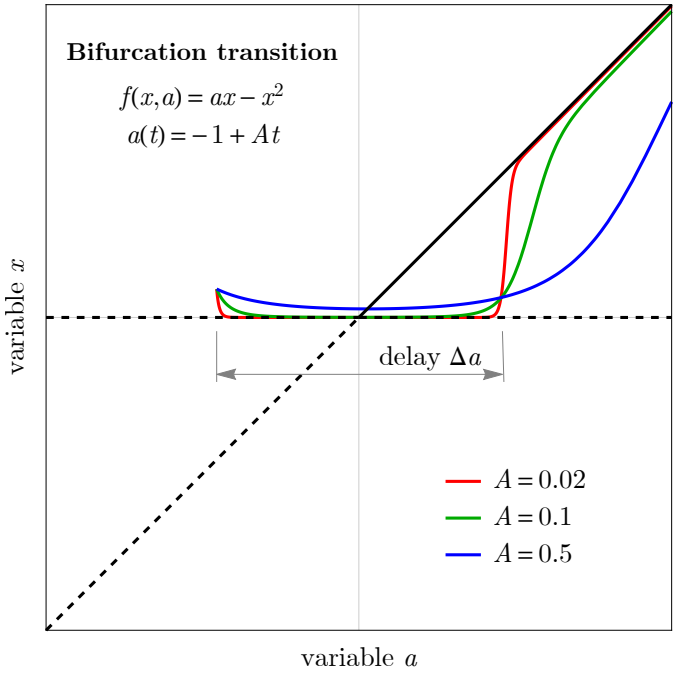

Figure 4: *The bifurcation transition diagram of the system (2.18) for different values of the parameter A with the initial condition $x_0 > 0$ close to zero. Note that A is a velocity ($\dot{a} = A$), so the solution for $A = 0.02$ approaches to the asymptote slower than the solution for $A = 0.5$ in real time; compare to figure 5.*

For the initial state shown in figure 4, the transition near the tipping point $(a, x) = (0, 0)$ is considerably delayed. For a small A, the solution is slowly varying until a jump transition to another slowly varying solution occurs. The value Δa between these two jumps is the delay of the bifurcation transition.

The time development of the solutions from figure 4 and their rate of change $\mathrm{d}x/\mathrm{d}a$ is shown in figure 5. The delay can be found from the peaks in the rate of change shown in 5b (e.g., for $A = 0.02$, it becomes $\Delta t = 101.895$ and $\Delta a = 2.0379$).

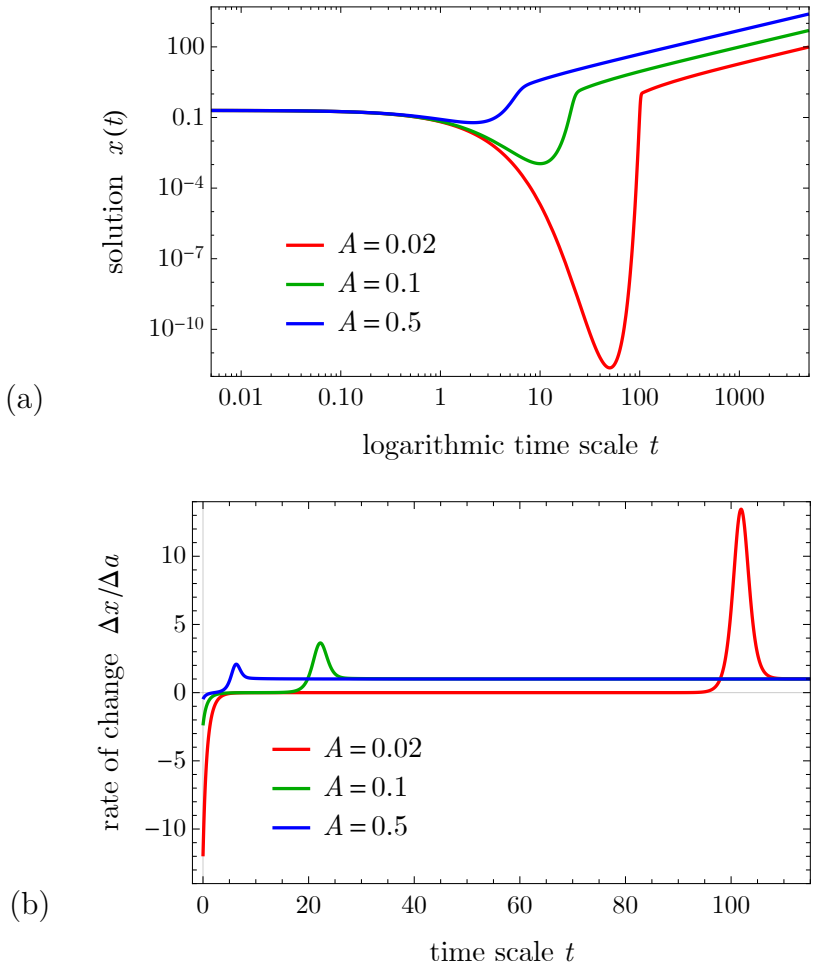

Figure 5: *The time development of (a) the solutions from figure 4, and (b) the rate of change* $\mathrm{d}x/\mathrm{d}a$ *for the same solutions.*

This simple toy model clearly shows a glimpse of properties which could be faced when giving time dependence to a single parameter (like the slow passage near an existing steady bifurcation point). In the following, we turn our attention to the real-world models for climate change, (1.9) and (1.10), and examine their bifurcation transitions.

3 Plan of the practical work

There are two steps to the practical work. The first step is to construct a bifurcation diagram for the system (1.9). Firstly we model albedo as a function of temperature. The function used for albedo will be a very simple one in terms of results. Consider the smooth nonanalytic function

$$f(x) = \begin{cases} 0, & x \leq 0, \\ \mathrm{e}^{-1/x}, & x > 0. \end{cases} \tag{3.1}$$

We use $f(x)$ to model a smooth transition function $g(x)$ as,

$$g(x) = \frac{f(x)}{f(x) + f(1-x)}, \tag{3.2}$$

which goes from 0 when $x \leq 0$ to 1 when $x \geq 1$ with a smooth transition in the interval $[0, 1]$. Finally we modify $g(x)$ to get,

$$\alpha(T) = (a_{\mathrm{w}} - a_{\mathrm{i}}) \cdot g\Big(T - (m - v)/(2v)\Big) + a_{\mathrm{i}}, \tag{3.3}$$

where a_{w} and a_{i} denote albedo of water and ice, respectively, m denotes the melting point of water, and $2v$ is the variance of how much it takes going from a_{t} and a_{w}.

After constructing the albedo function $\alpha(T)$ the bifurcation diagram can be constructed. The roots of equation (1.6) are the same as when solving (1.9) as a differential equation numerically letting $n \to \infty$. The roots are solved for ΔF in some undetermined interval. Since the conditions for when the solution is stable or unstable is known the bifurcation diagram may be plotted using a solid line or a dashed line respectively.

The second step is to make the bifurcation parameter a function changing with time. This step will be done in a similar fashion to section 2.4. Using ΔF as a function of time $\Delta F(t)$ a time-dependent bifurcation transition diagram will be created for three values of ϵ. The time-dependent bifurcation transition diagram will be constructed for several variants of $\Delta F(t)$:

$$\Delta F(t) = \Delta F_0 + \epsilon\, t, \qquad \text{linear}, \tag{3.4a}$$
$$\Delta F(t) = \Delta F_0 + \epsilon\, t^2, \qquad \text{quadratic}, \tag{3.4b}$$
$$\Delta F(t) = \Delta F_0 + \epsilon\sqrt{t}, \qquad \text{sublinear}, \tag{3.4c}$$
$$\Delta F(t) = \Delta F_0 + \epsilon \log(1 + t), \qquad \text{logarithmic}. \tag{3.4d}$$

After solving (1.10) and noting the values for $\Delta F(t)$ and $T(t)$ for the different values ϵ for each variant of $\Delta F(t)$, the time-dependent bifurcation transition diagram will be created whose results will be analysed.

4 Results of the practical work

We consider the equation (1.9) with the parameters $S = 1360.8\,\mathrm{W\,m^{-2}}$, $\lambda = 0.612$, and $\bar{C}_p = 1\ \mathrm{J\ K^{-1}m^{-2}}$.[1] The albedo function (3.3) is shown in figure 6 with the parameters $a_\mathrm{w} = 0.3$, $a_\mathrm{i} = 0.55$, $m = 273.15\,\mathrm{K}$, and $v = 10\,\mathrm{K}$. Two example solutions of (1.9) for $\Delta F = 0$ are shown in figure 7. The roots of the equation (1.6) give the fixed points for (1.9), and the bifurcation diagram is shown in figure 8. We observe two stable steady-state solutions and one unstable. We can identify two tipping points, $(21.72, 267.2)$ and $(-25.52, 278.9)$, in the interval $\Delta F \in [-30, 30]$.

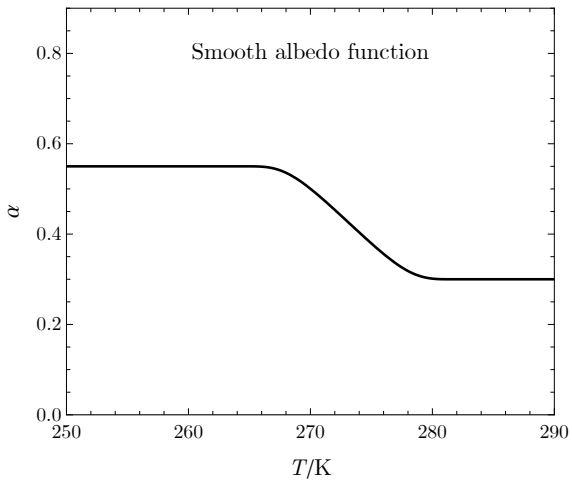

Figure 6: *Albedo function (3.3).*

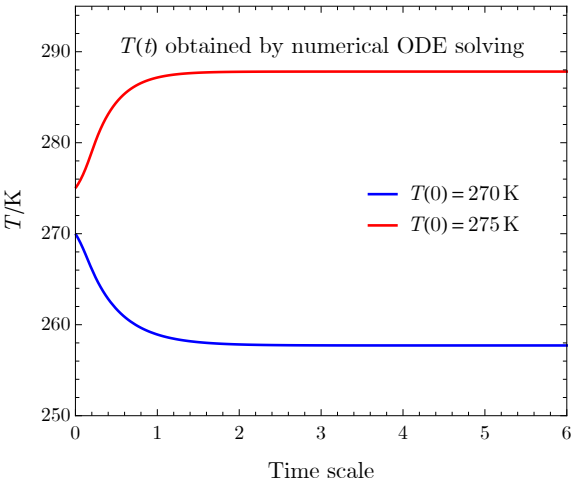

Figure 7: *Two sample solutions of (1.9).*

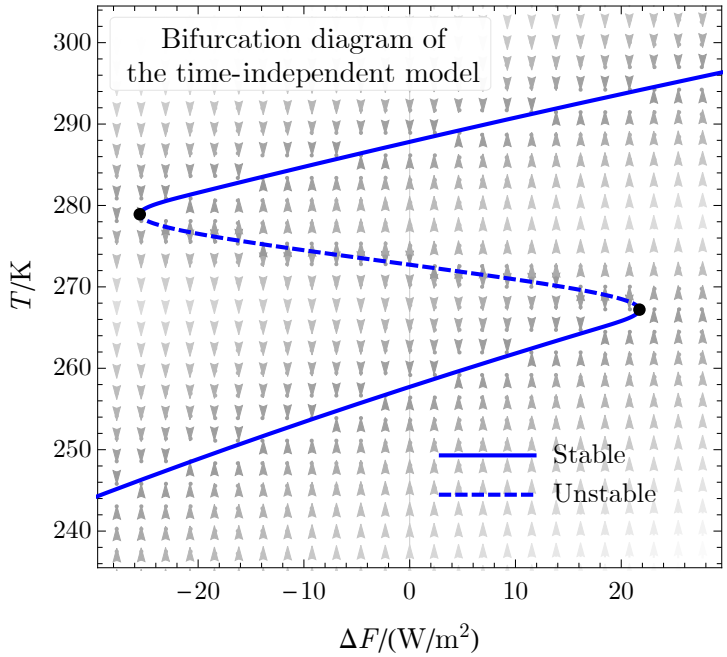

Figure 8: *The bifurcation diagram for the time-independent model (1.9).*

[1] Note that for the atmosphere $\bar{C}_p = 1.02 \times 10^7\ \mathrm{J\ K^{-1}m^{-2}}$ so the real-time scale is $\approx 10^7$ bigger.

The stream plot of the model (1.9) with constant ΔF is shown in figure 9 panel (a). Therein any solution eventually tends to an equilibrium as t goes to infinity; e.g., at $\Delta F = 0$, the temperature approaches the lower equilibrium for $T(0) = 270\,\mathrm{K}$, while it approaches the upper equilibrium for $T(0) = 275\,\mathrm{K}$. Things, however, become more complicated for the time-dependent model (1.10), whose stream plots are shown for different kinds of $\Delta F(t)$ in the other panels of figure 9.

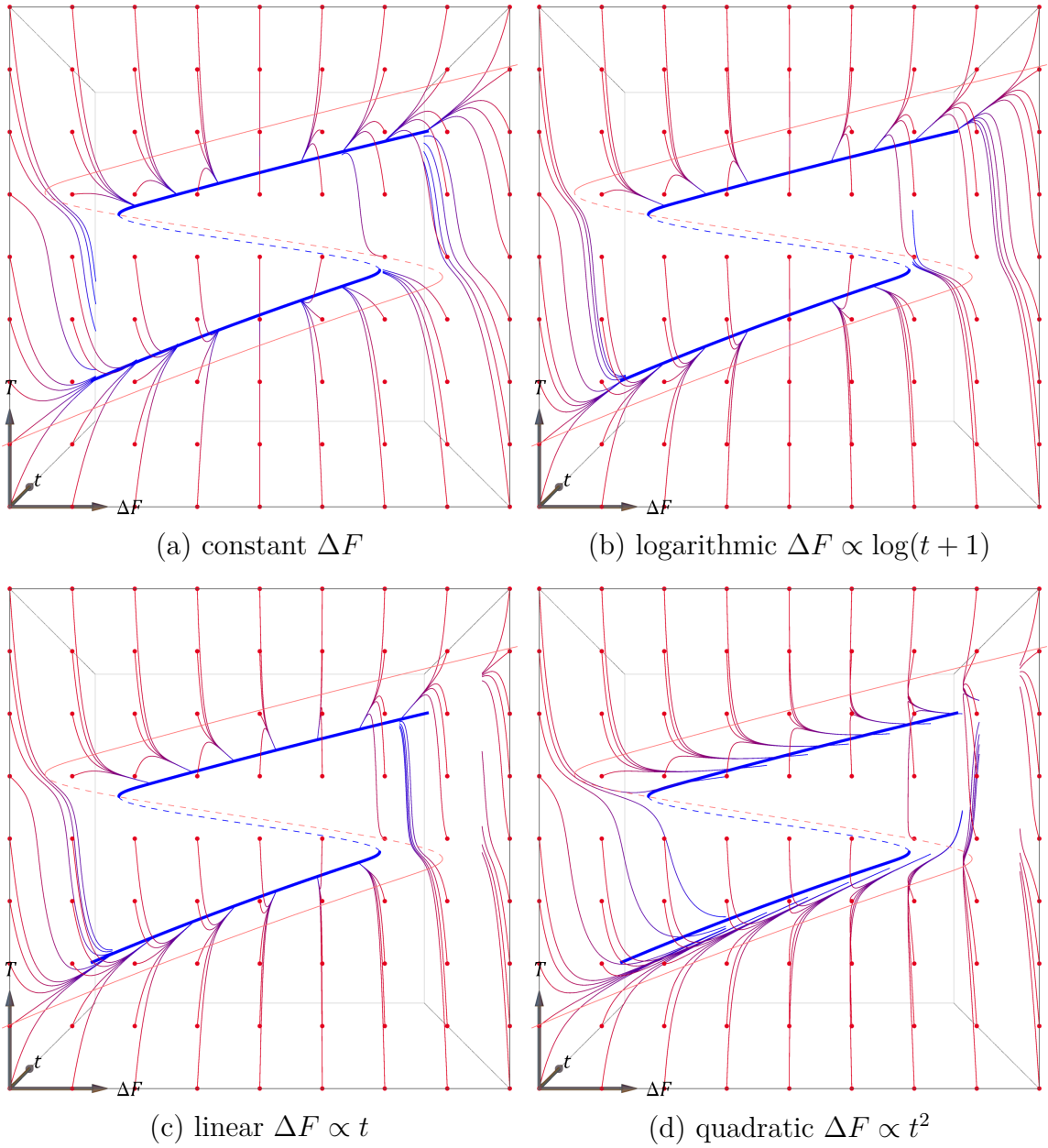

(a) constant ΔF (b) logarithmic $\Delta F \propto \log(t+1)$

(c) linear $\Delta F \propto t$ (d) quadratic $\Delta F \propto t^2$

Figure 9: *3D stream plots for the extended model (4.1) using a perspective projection where the depth is along t. The objects closer to $t = 0$ are depicted in red while farther objects at later t are given in blue. Observe how fast the solutions drift to the right (towards larger ΔF) for different variants of $\Delta F(t)$.*

The stream plots in figure 9 are obtained by promoting ΔF and t to state variables, then introducing another independent variable τ and setting $\mathrm{d}t/\mathrm{d}\tau = 1$. This gives an autonomous system with the state variables $(T, \Delta F, t)$,

$$\frac{\mathrm{d}T}{\mathrm{d}\tau} = \frac{1}{\bar{C}_p}\left[\frac{1}{4}S\left(1-\alpha(T)\right) - \lambda\sigma T^4 + \Delta F\right], \qquad \frac{\mathrm{d}\Delta F}{\mathrm{d}\tau} = \varphi(t), \qquad \frac{\mathrm{d}t}{\mathrm{d}\tau} = 1. \tag{4.1}$$

Here, $\varphi(t) =$ is a derivative of $\Delta F(t)$, i.e., $\varphi(t) = \Delta F'(t)$, where $\Delta F(t)$ is one of the variants from (3.4). This way, (4.1) becomes equivalent to (1.10). For example, an integral of $\varphi(t) = \epsilon/(1+t)$ will give $\Delta F = \Delta F_0 + \epsilon \log(1+t)$. Three dimensional stream plots of (4.1) from figure 9 are then straightforward. Note that the stream plots provide only qualitative analysis; for instance, one can observe 'how' the solutions drift to larger vales of ΔF for different variants of $\Delta F(t)$. A more detailed numerical analysis is required around the bifurcation points.

In particular, we focus on the lower tipping point as it is the one of interest for global warming and specifically for an *increase* in greenhouse gases. We also begin to look at different cases where ΔF is a function of time in a more detail. The same initial ΔF_0 will be used for all variants of ΔF; it has be found that the best results are obtained for $\Delta F_0 = 20$. The different values used for ϵ were $0.5, 1$, and 1.5 for all cases in (3.4).

4.1 Linear $\Delta F(t)$

The solution to the differential equation (1.10) using the linear variant of $\Delta F(t)$ are shown in figure 10. The plots are for the initial condition $T(0) \approx 265.808$ K.

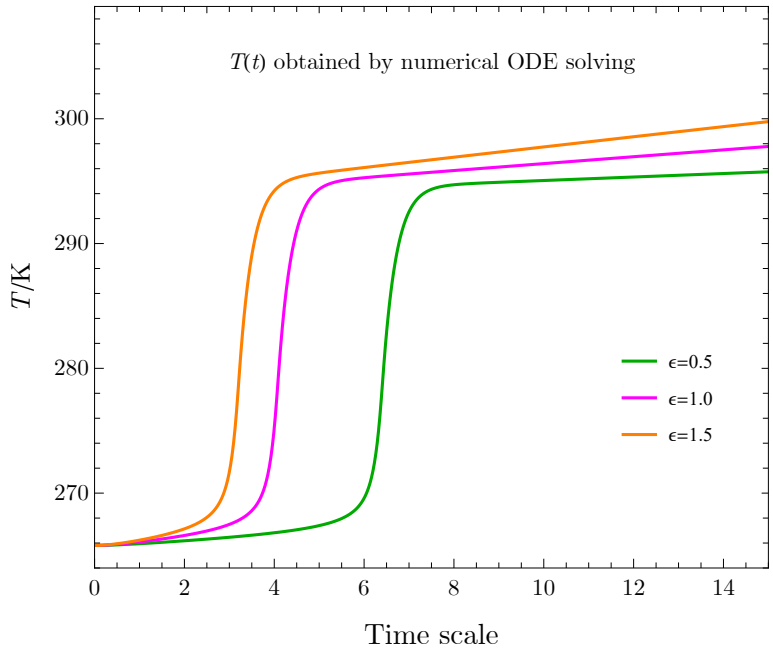

Figure 10: *Solutions to ODE (1.10) using* $\Delta F(t) = 20 + \epsilon t$.

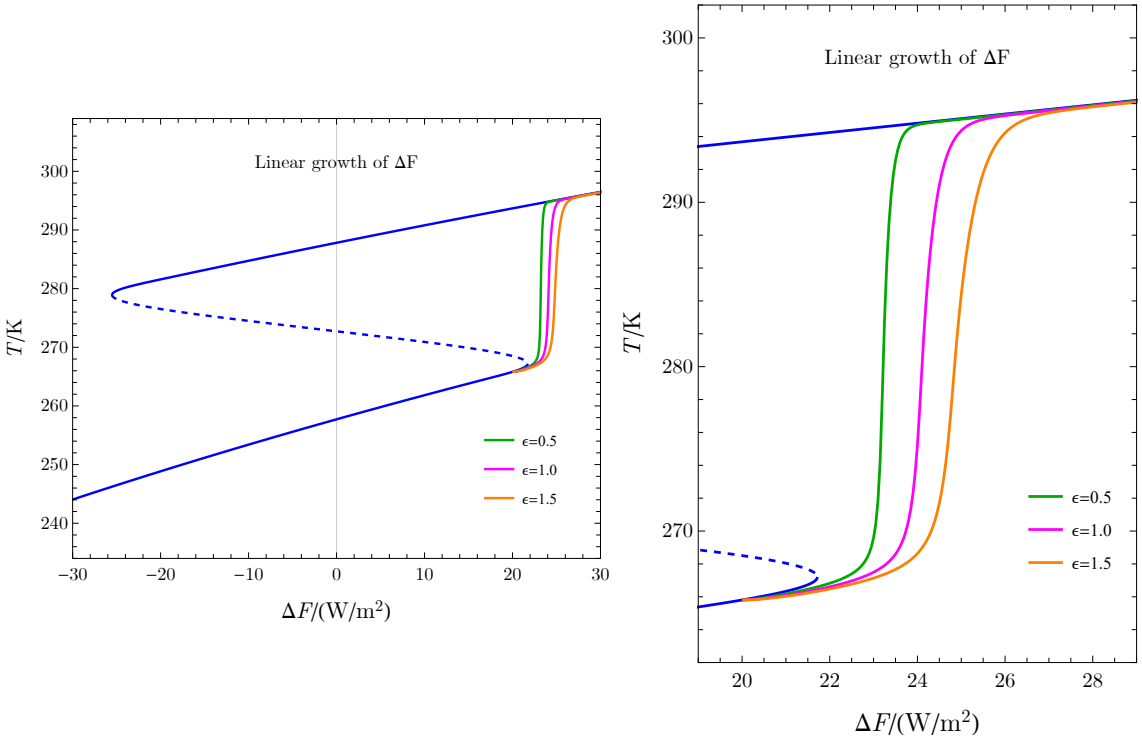

Figure 11: *The bifurcation transition diagram of* (1.10) *for* $\Delta F(t) = 20 + \epsilon t$. *The right figure zooms in on the lower tipping point where the transition is easier to view.*

At first, the result looks as expected; faster speed of growth for ΔF contributes to faster growth of T. Obtaining the values for ΔF and the corresponding T for the bifurcation transition diagram in figure 11 mirrors the behaviour found in section 2.4. Even though $\epsilon = 0.5$ increases ΔF by a slower rate than $\epsilon = 1.5$ the rate at which T 'tips' is quicker in comparison. In other words the qualitative change is quicker while the temperature rises slowly.

4.2 Quadratic, sublinear and logarithmic $\Delta F(t)$

The different growths of ΔF such as quadratic, sublinear, and logarithmic behave the same way as the linear variant and mirror the results from linear growth. The respective plots are shown in figures 12, 13, and 14, which should be compared with figure 11. The comparison for each of figures 11, 12, 13, and 14 may be viewed in figure 15. For each type of growth (quadratic, sublinear, and logarithmic), while the speed of growth indeed matches the growth for T the qualitative change of the steady-state solution is faster when the speed of growth is slower.

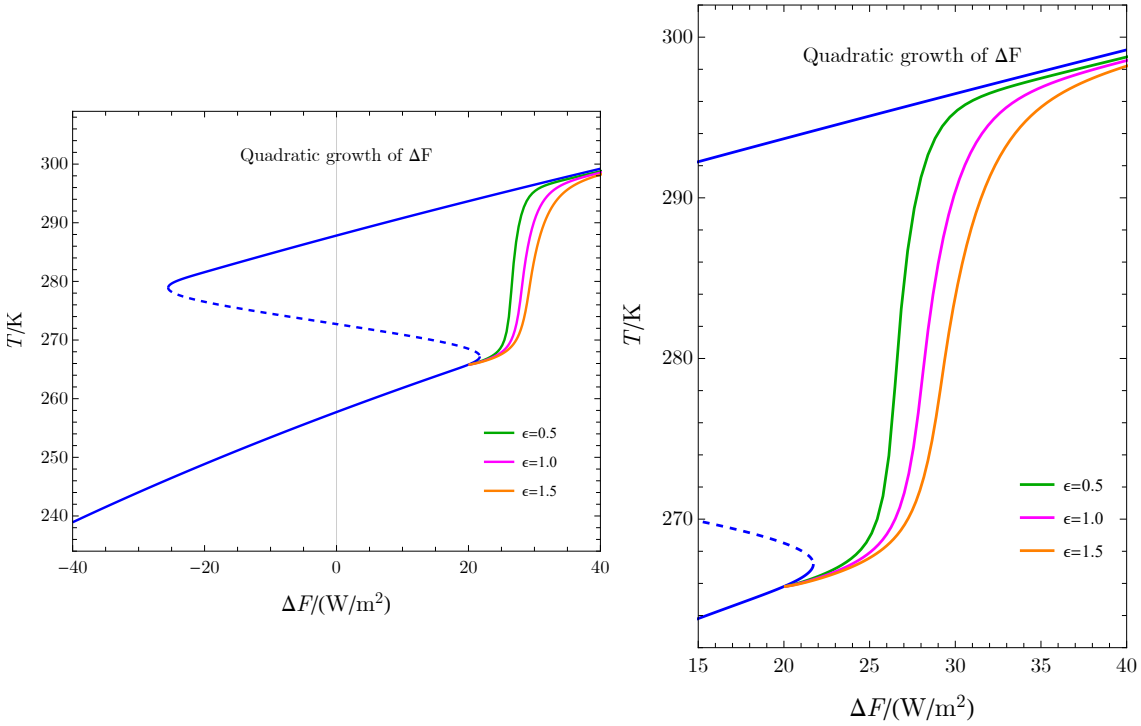

Figure 12: *The bifurcation transition diagram of* (1.10) *for* $\Delta F(t) = 20 + \epsilon t^2$.

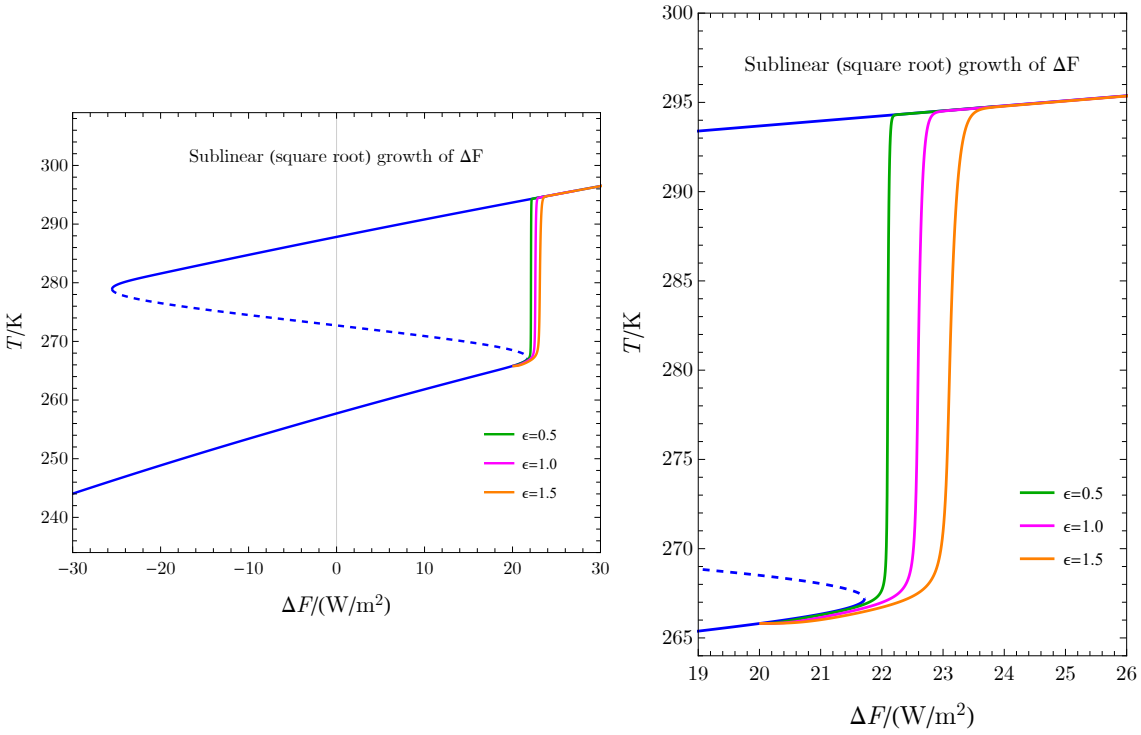

Figure 13: *The bifurcation transition diagram of* (1.10) *for* $\Delta F(t) = 20 + \epsilon\sqrt{t}$.

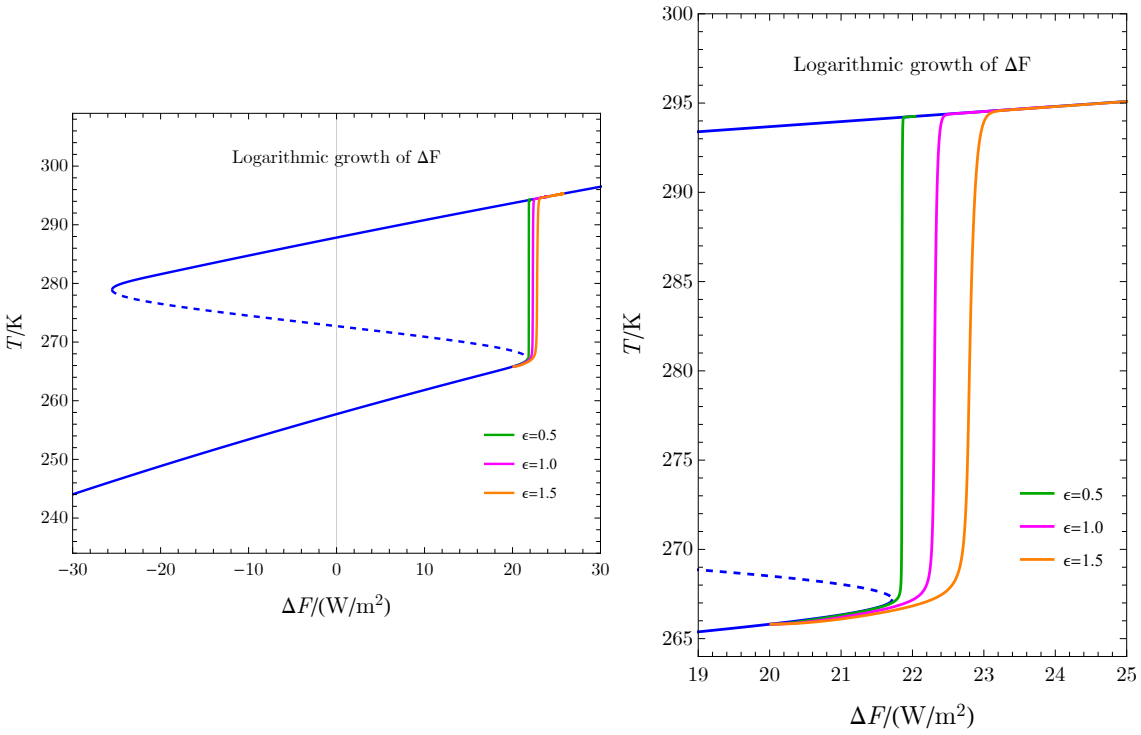

Figure 14: *The bifurcation transition diagram of* (1.10) *for* $\Delta F(t) = 20 + \epsilon \log(1+t)$.

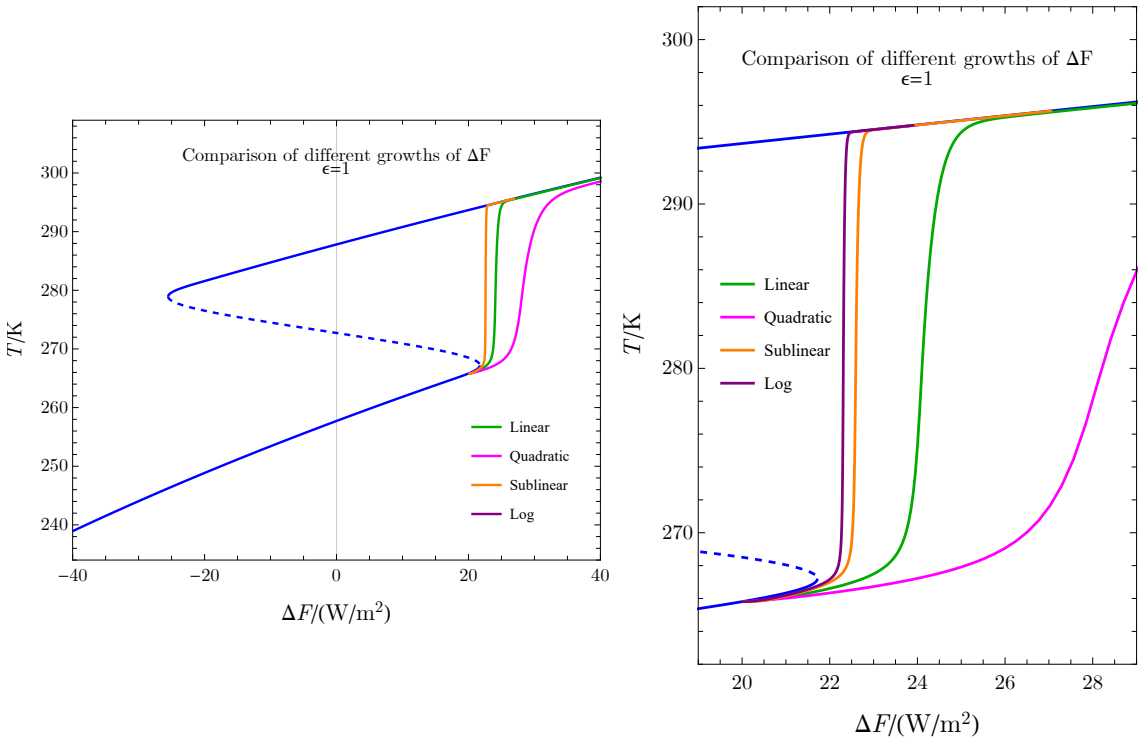

Figure 15: *The bifurcation transition diagram of* (1.10) *comparing the different rates of growth. The value for* ϵ *is* 1 *for all rates of growth.*

4.3 Tipping point prevention

One interesting issue to pursue is whether it is possible to prevent the system from reaching the tipping point; in particular, to check if reversing the greenhouse effect could prevent the tipping point to be reached. For this discussion the variant of ΔF which will be used is $\Delta F(t) = 20 + a\sqrt{t} - t$ for four different values of a. The upper and lower values used for this purpose are $a = 2.8$ and $a = 3.0$, while the middle value is intentionally a very small change in the 10^{-30} position. The result is given in figure 16; it shows that there is a possibility that the tipping point may be avoided. In the case when the tipping point is reached and ΔF continues to decrease one finds that the system eventually reaches the other tipping point. Nonetheless, if the decrease is powerful enough then there is a chance the system will not end up past the critical point.

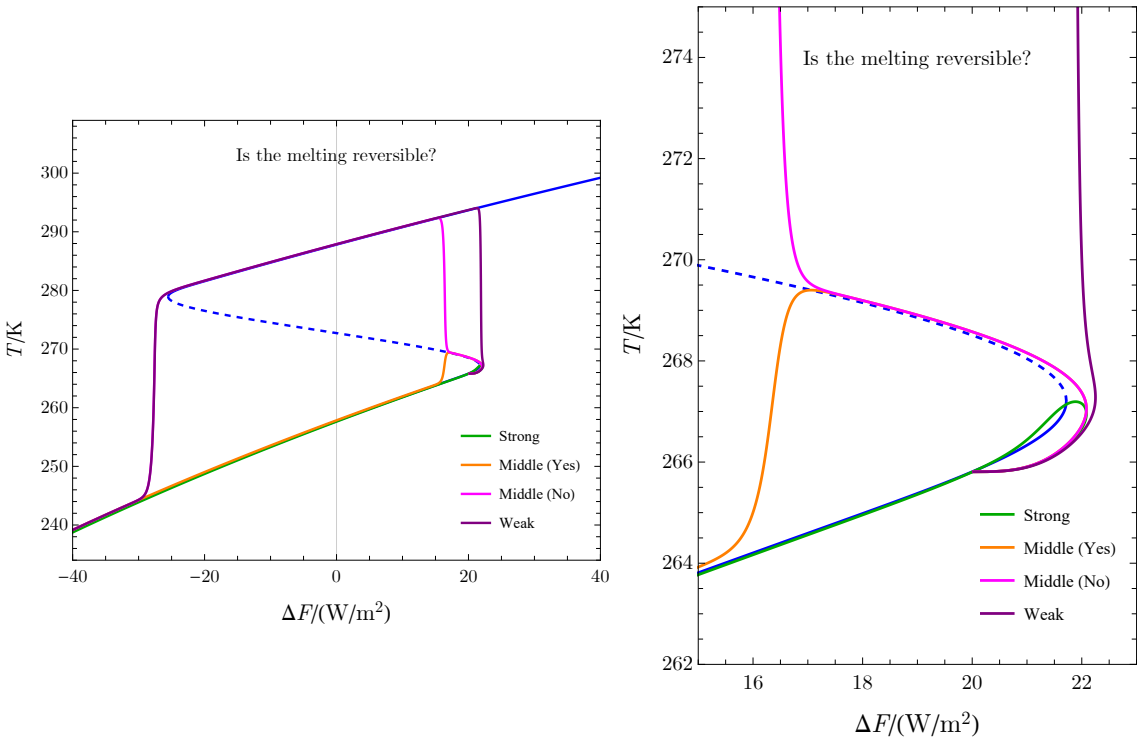

Figure 16: *The bifurcation transition diagram of (1.10) for $\Delta F(t) = 20 + a\sqrt{t} - t$. The label 'strong' indicates that the linear term is stronger than the sublinear term, giving a reversible increase of greenhouse gases which does not go past the tipping point. Similarly for weak, except the linear term is weaker than the sublinear term leading to the system being pushed past the tipping point. The two middle plots show the case when the system is very close to tipping, and how a small difference in the 10^{-30} position may cause the system to be pushed past the tipping point.*

5 The numerical code

The solving equations and printing of the bifurcation diagram was initially done in Python. The Python code handles the time-independent bifurcation diagram, whose values are printed out to a csv-file. The code for the smooth albedo function and model (1.9) were directly adapted as Python functions. The program first finds the points of extrema on the graph only used to find the amount of extrema points. Then it takes an interval, which in this case is $[-30, 30]$, splits it up into a set of numbers with equal difference (in this case 0.01) and for each element in the set finds the roots of the model. First, the program guesses where the roots of the model might be for each $\Delta F \in [-30, 30]$, then it computes the root using the secant method with accuracy in the 10^{-9} position. Since there is more than one root in some cases (we are expecting three at most) we need to place the roots in such a way that they match the location of the previous root. This is done by just checking how many solutions there are and placing the roots in the correct list. Then all of the lists are exported into a csv-file which may be read by a different program for plotting. Note that the code only works for saddle-node bifurcations with at most three roots. It can be easily modified to hold more than three roots though.

The decision to start using Mathematica was quickly made after the first coding, since Python's plotting library seemed not as versatile. Also, Mathematica is much easier to work with, when doing experiments with numerical methods. The first Mathematica notebook was made to solve and export the values for model (1.10). Using Mathematica built-in function `NDSolve` the solution to the ordinary differential equation (1.10) are obtained. Then the values of $\Delta F(t)$ and $T(t)$ are written in a separate csv-file for the three values of ϵ. This is done for all variants of ΔF mentioned in section 3.

A second Mathematica notebook was made to combine the csv-files into a single plot and compare the results. This code is responsible for the figures 6 to 16 except for figure 8. Since section 2 also needed plots to show the results in a tidy way a third Mathematica notebook was created, which is more extensive and contains the vector plots to showcase the bifurcation diagrams for saddle-node and transcritical bifurcation. Further, the notebook also contains a vector field plot (using `VectorPlot`) and a streamline plot (using `StreamPlot`) for the non-autonomous ODE variant of (2.13) and the bifurcation transition diagram for three values of $A \in \{0.02, 0.1, 0.5\}$ in (2.17). Afterwards the program plots the solution to (2.18) using a logarithmic time scale and also plot the rate of change $\Delta x/\Delta a$.

As an aid in qualitative analysis, it was decided to make the 2D bifurcation and 3D bifurcation transition diagrams for the models (1.9) and (1.10), respectively. The 2D bifurcation diagram for (1.9) was plotted using Mathematica's built-in functions `VectorPlot`; this made much of the initial Python code obsolete for plotting purposes. The 3D bifurcation transition diagrams were made using the `StreamPlot4D` package, which gives a nice representation of how T changes with increasing ΔF and t along with the time-independent bifurcation diagram.

The code of the practical work is publicly available [14]; here the previously mentioned Mathematica notebooks are combined into one comprehensive notebook.

6 Discussion and conclusion

This section includes a small discussion on the results and some flaws on the execution on which then can be further investigated using better tools. Finally a conclusion is made, assuming for of course the results and the imperfections which may have impacted the results.

6.1 Discussion

The results are quite worrying, if applicable. The temperature increase is already identified to be a bad scenario for the Earth system, but a slower increase of temperature implies a faster rate of change once the system is pushed past the critical point. Even then, the different types of growth still confirm the same hypothesis that a slower change of temperature implies a faster rate of change for the system. More specifically, the time scale is the same for the different growths of temperature once the system reaches the tipping point.

Furthermore, the reversible results were not initially planned to be done as part of the practical work; these came later on, after concluding that the fast temperature change is not good at all for climate change, but the alternative slow temperature change will imply a faster rate of change once the system is pushed past the critical point. Ideally, the system should not be pushed past the tipping point at all. The problem with the plan to decrease greenhouse gases is that the plan cannot be immediately effective. In a hypothetical scenario where the decrease of greenhouse gases is powerful enough it may be possible to not push the Arctic sea-ice past the tipping point. Right now, such a scenario seems unlikely; it is more probable that the system is being pushed past its critical point.

The above discussion may suggest a doomsday scenario for the Earth. Fortunately there are two silver linings which suggests that the results may not be entirely applicable. The first is about the function used for albedo. The used albedo function is a very simple with a smooth change between two values and nothing more. It represents the albedo decently accurate, but the used numbers may be completely wrong. The second silver lining is the fact that equation (1.9), which has been used as the model for the Arctic sea-ice, is not entirely applicable either; the model works better for the Earth as a whole rather than just a specific location on the Earth. The model is a good enough estimate of the real-life scenario, but it misses key factors which definitely impact the speed at which the Arctic sea-ice melts.

Does that mean all of the work done is not applicable? That may not be the case looking at what already happened on the Greenland ice-sheet thousands of years ago. After a period called the Younger Dryas event several thousands of years ago the Earth suddenly experienced an abrupt climate change whose results directly affected the Greenland ice-sheet [15]. The Greenland climate among several other regions around the world at the time experienced sudden warmth which marked the end of the ice age. Analysis of the Greenland ice core reveals that the temperature graph from the Greenland climate several thousands of years ago very closely resembles a type of bifurcation, which may be viewed in figure 17.

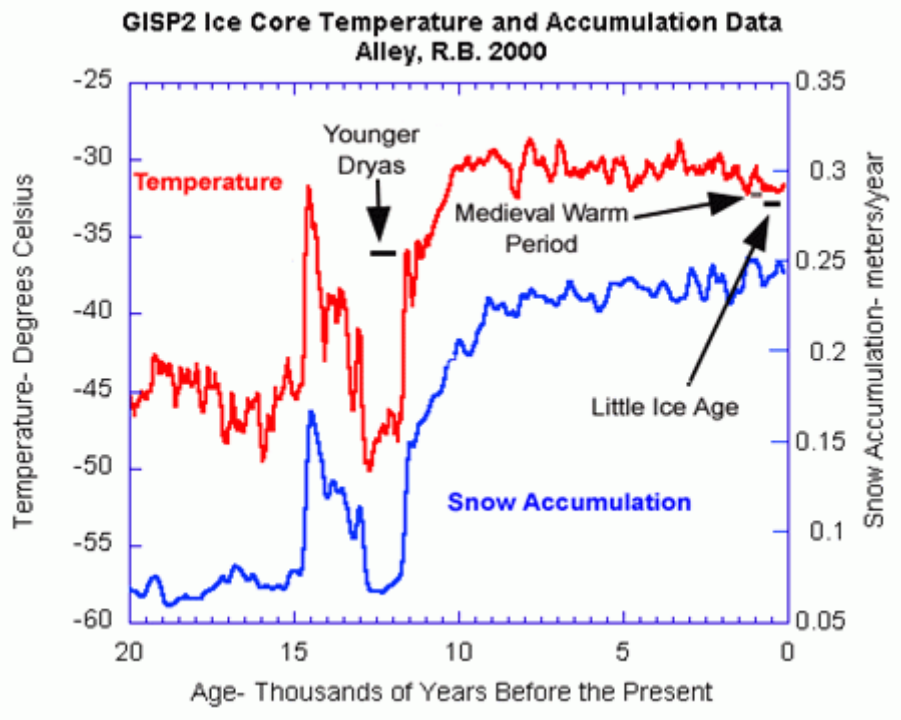

Figure 17: *Greenland climate data from Richard B. Alley [16]. The plot shows ice core temperature and accumulation data on the GISP2 site in Greenland.*

6.2 Conclusion

To conclude, the end result for the Arctic ice sheet is rather tricky to evaluate. In isolation, the melting of the Arctic sea-ice is a concern due to the tipping point explained by ice-albedo positive feedback. If the temperature continues to rise due to global warming, then regardless of how quickly the temperature rises, once the Arctic sea-ice system is pushed past the critical point, the melting will only continue in a similar time window. The immediate obvious approach, which is to slow down the global warming, can be a valid solution, but if done too late, then the melting will not stop. It is very likely that we have to prepare for a sudden climate change in the near future. The Arctic sea-ice, whose end result is complete melting of the sea ice, is just one of many subsystems of the Earth susceptible to global warming and may cause ripples into other subsystems.

References

[1] T. M. Lenton, H. Held, E. Kriegler, J. W. Hall, W. Lucht, S. Rahmstorf et al., *Tipping elements in the earth's climate system*, *Proceedings of the National Academy of Sciences* **105** (2008) 1786–1793.

[2] P. Hewitt, *Conceptual Physics*. Pearson Education, 2007.

[3] K. McGuffie and A. Henderson-Sellers, *A Climate Modelling Primer*. John Wiley & Sons, 2005.

[4] M. I. Budyko, *The effect of solar radiation variations on the climate of the earth*, *Tellus* **21** (1969) 611–619.

[5] W. D. Sellers, *The Energy Balance of the Atmosphere and Climatic Change*, *Journal of Applied Meteorology* **3** (06, 1964) 337–339.

[6] W. D. Sellers, *A Global Climatic Model Based on the Energy Balance of the Earth-Atmosphere System*, *Journal of Applied Meteorology* **8** (06, 1969) 392–400.

[7] W. D. Sellers, *A New Global Climatic Model*, *Journal of Applied Meteorology* **12** (03, 1973) 241–254.

[8] G. Kopp and J. L. Lean, *A new, lower value of total solar irradiance: Evidence and climate significance*, *Geophysical Research Letters* **38** (2011) .

[9] NIST. CODATA recommended values (2018), accessed 2020-08-05, https://physics.nist.gov/cgi-bin/cuu/Value?sigma|search_for=Boltzman.

[10] D. Zwillinger, *Handbook of Differential Equations*. Academic Press, 1997.

[11] P. L. Sachdev, *Nonlinear Ordinary Differential Equations and Their Applications*. Taylor and Francis, 1990.

[12] D. Jordan and P. Smith, *Nonlinear Ordinary Differential Equations: An Introduction for Scientists and Engineers*. OUP Oxford, 2007.

[13] E. W. Weisstein. "Erfi." From MathWorld, accessed 2020-08-05, A Wolfram Web Resource: https://mathworld.wolfram.com/Erfi.html.

[14] M. Kocic. "Time-Dependent-Bifurcation" from GitHub, accessed 2020-08-16, https://github.com/Unoriginal0/Time-Dependent-Bifurcation.

[15] R. B. Alley, *The Two-Mile Time Machine: Ice Cores, Abrupt Climate Change, and Our Future*. Princeton University Press, 2002.

[16] R. B. Alley, *The younger dryas cold interval as viewed from central greenland*, *Quaternary Science Reviews* **19** (2000) 213 – 226.